

# Performance evaluation of dynamic voltage restorer using bidirectional impedance converter with UCAP

A. Anitha<sup>1</sup>, K. C. R. Nisha<sup>2</sup>

<sup>1</sup>Department of Electrical and Electronics Engineering, New Horizon College of Engineering, Visvesvaraya Technological University (VTU), Belagavi, India

<sup>2</sup>Department of Electronics and Communication Engineering, New Horizon College of Engineering, Visvesvaraya Technological University (VTU), Belagavi, India

## Article Info

### Article history:

Received Feb 26, 2025

Revised Oct 31, 2025

Accepted Dec 11, 2025

### Keywords:

Bidirectional converter

Bidirectional ZSI

DC link control

Dynamic voltage restorer

MPC

UCAP

## ABSTRACT

With the involvement of renewable energy sources, plug-in hybrid automobiles, and fault occurrence, power quality has degraded nowadays. The most effective device utilized in distribution systems to enhance power quality is the dynamic voltage restorer (DVR). For deep sags, DVR with storage topology is more beneficial, although it has challenges with converter and storage element rating. To address this, various converters and energy storage elements like ultracapacitors are reviewed. In this paper, a DVR with an ultracapacitor (UCAP) using an impedance bidirectional converter is simulated, and power quality indices are compared with VSI-BDC. The simulation result reflects the enhanced capability of the suggested DVR in a wide range of operations, improved power quality indices, and its effectiveness in swell conditions. The control of DC link voltage with PI and model predictive control (MPC) were simulated and compared.

This is an open access article under the [CC BY-SA](https://creativecommons.org/licenses/by-sa/4.0/) license.



## Corresponding Author:

A. Anitha

Department of Electrical and Electronics Engineering, New Horizon College of Engineering

Visvesvaraya Technological University (VTU)

Belagavi, India

Email: anithanelson24@gmail.com

## 1. INTRODUCTION

In the recent past, the quantity of critical loads—like medical equipment in clinics, prisons, and school. This have increased dramatically, raising significant concerns about the power quality of these delicate loads. Rapid occurrences like transients, voltage impulses, faults, voltage swells and sags, high-frequency noise, and complete power loss can all be signs of poor power quality. As a result, this situation leads to significant financial losses, decreased productivity, outages of critical and sensitive loads, as well as data loss. The primary issues with power quality are voltage sags, fluctuations, voltage swells, harmonics, transients, flickers, and interruptions. A reduction in the root-mean-square (RMS) voltage between 0.1 and 0.9 pu is known as voltage sag during 0.5-30 cycles. Due to various reasons such as faults, starting of large loads, supply voltage variations, grid loading, starting current, and voltage rise or fall, voltage sag or dip is caused. It causes lock-up, motor overload or stalling, and misleading data. An increase in RMS voltage between 1.1 and 1.8 pu during 0.5 to 30 cycles is known as voltage swell. Voltage swell is due to the start/stop of heavy loads and supply variations. It causes data loss and damage to equipment. Voltage sags are the most serious and common problems with power quality in the contemporary power system, and DVR is the most economical way to reduce them [1].

Dynamic voltage restorer (DVR) topologies have been the subject of an ongoing search due to a number of factors, including the desire to increase device economics and technical performance, efficiency, and

incorporation of new technologies [2]. Soomro *et al.* [3] proposes DVRs without stored energy, enabling direct conversion of AC-AC using sliding mode control. The performance and cost of several DVR topologies, both with and without energy storage, are examined [4], and the stored energy topology is recommended despite its complexity and expense.

Many researches have been done in recent years to improve DVR operating performance and reduce expenses with stored energy. A variety of rechargeable energy storage technologies based on batteries (BESS) and superconducting magnets (SMES), ultracapacitors, and fuel cell integrated DVRs are examined using various control and compensation techniques to enhance the quality of power [5]-[8]. Compared to all, ultracapacitors (UCAPs) have emerged as a viable substitute due to their long cycle life, quick charge/discharge capabilities, and high-power density compared to batteries. Shah *et al.* [9] proposes new sliding mode control for UCAP-integrated DVR. To effectively use UCAPs with a DVR, a DC-DC bidirectional converter is essential to connect the UCAP bank with the DC link of the voltage source inverter (VSI). A voltage source inverter needs an additional converter to boost the voltage, which increases the cost.

Thus, the topologies of bidirectional converters have undergone extensive research and optimization recently for various applications [10]. To obtain a wide range of voltages and eliminate short circuit problems, impedance source inverters are recommended [11]. To develop bidirectional DC-DC converters with a wide voltage conversion range appropriate for integrated energy storage systems, both isolated converters based on transformers and non-isolated converters based on impedance networks are being investigated. Impedance-source inverters (ZSI) are used in services like low-voltage ride through (LVRT) and adjustment of reactive power, grid integration, and electric vehicles [12]-[15]. Z-source inverter pulse width modulation approaches are analyzed [16]. The performance outcomes of DVR's enhanced strategy are discussed [17], [18]. The isolated bidirectional converter topologies are used in DVR to compensate sag and swell [19], [20].

The authors of the paper [21] proposed a self-tuned fuzzy controller that is comparable to the PI regulator technique for DVR control. The application of fuzzy logic-based PI in systems such as custom power devices is limited by the membership function's formulation. The control algorithm was modified by Naidu *et al.* [22] for DVR control, and it produced an agreeable result in multi-disturbance compensation. Tuning of PI controller in DVR using the least mean square (LMS) method, optimization algorithm was discussed in the literature [23], [24]. Recent research on model predictive control gives better optimization results than PI controllers [25].

In this paper, the benefits of DVR and UCAP, a bidirectional impedance source inverter, are combined. It focuses on how a bidirectional impedance converter with an ultracapacitor might improve DVR performance. Due to their low energy density and high-power density, UCAP can handle higher power levels for longer periods of time, which can reduce sags and swells. When these energy storage components are included, grid failure is eliminated. Simulation using a PI and model predictive control (MPC) controller was also explored.

## 2. METHOD

### 2.1. Conventional DVR system

The DVR schematic for a low-voltage network is displayed in Figure 1. When a supply-side voltage disturbance occurs, the DVR, a power electronic device, responds by injecting the necessary voltage at the load side. Additionally, DVR mitigates supply-side disruptions for significant and sensitive loads. Typical DVR configurations consist of an energy storage unit linked to a DC-link capacitor, output filter, injection transformers, and a VSI [19].

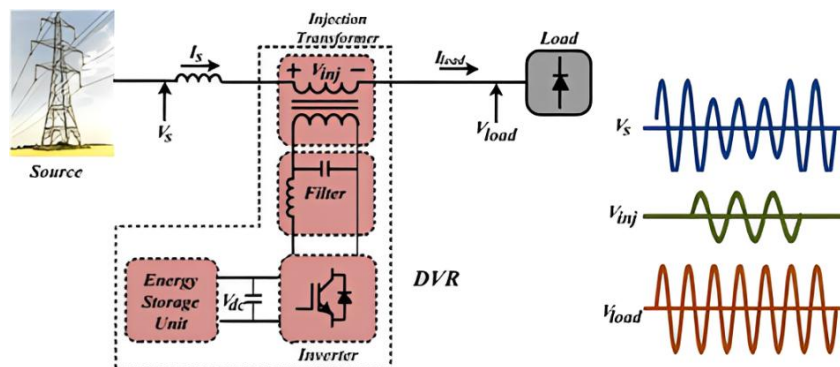


Figure 1. Conventional DVR system

The load voltage, supply-side voltage, and injected voltage could be related according to (1).

$$V_{load} = V_s + V_{inj} \quad (1)$$

DVR systems can take advantage of direct energy storage methods like SMES, batteries, or ultracapacitors. With their high responsiveness and long lifecycle, UCAPs are outperforming traditional storage in short-duration, high-power applications. Similar to a battery, a UCAP's voltage profile changes as it releases energy, hence it cannot be directly connected to the DC link of the inverter. To retain the DC-link voltage steady, a bidirectional DC-DC converter serves as an interface between UCAP and VSI. This study [7] uses a bidirectional DC-DC converter that functions as a buck converter while charging the UCAP from the grid and as a boost converter when releasing power from the UCAP. Average current mode control, which has been well examined in the literature, is used to regulate the output voltage of the bidirectional DC-DC converter in both buck and boost modes when charging and discharging the UCAP bank.

Output DC link voltage  $V_{out}$  and reference voltage  $V_{ref}$  are compared in average current mode control [7] displayed in Figure 2, and a voltage compensator receives the error after that provides a reference value for current ( $I_{uref}$ ). The control signals are then sent through a current compensator, which generates the pulses for the switches. Thus, the necessary voltage is injected during sag and absorbed during swell. The converter's rating can be computed as (2).

$$S_{power} = |1 - a| \quad \text{where } a = \text{sag depth} \quad (2)$$

The operational range and efficiency of these converters are not substantially enhanced. Although a VSI with bidirectional capability provides significant flexibility, such as grid support, regenerative braking, and energy storage it is associated with several drawbacks, including higher cost, reduced efficiency, complex control requirements, stability concerns, and the necessity for bulky passive filters.

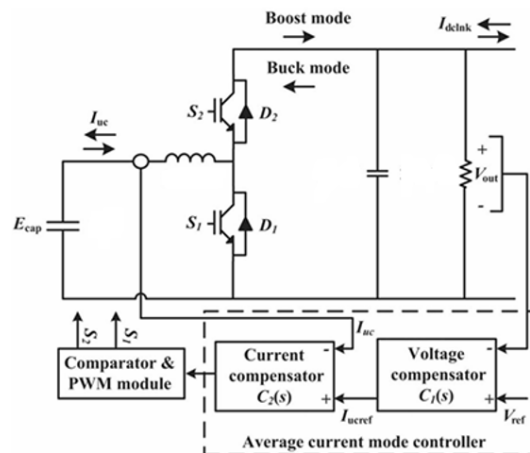


Figure 2. BDC with average current mode control

## 2.2. Proposed model

Impedance source inverters can operate efficiently even when the input voltage varies widely (as in the case of UCAP), and they eliminate the need for an additional converter and a DC-link capacitor. Reliability is improved by utilizing the shoot-through states. To extend the operating range, enhance effectiveness, and reduce stress on the switches, a ZSI-based bidirectional inverter is proposed, as shown in Figure 3.

To mitigate all forms of voltage sag and swell across a wide operating range, a UCAP and a DVR are integrated using a ZSI. A distinct feature of the ZSI is the shoot-through state, an additional switching mode that enables voltage boosting. In this state, the top and bottom switches of the same inverter leg are turned on simultaneously, which effectively short-circuits the load terminals. Unlike in a conventional VSI (where this would cause damage), the impedance network of the ZSI safely handles shoot-through and boosts DC-link voltage. The ZSI increases the DC voltage during the shoot-through interval ( $T_{shoot}$ ). The boost factor can be adjusted by varying the shoot-through duration. In the simple boost control method, the shoot-through period is generated by comparing a triangular carrier waveform with two constant DC reference voltages. This produces the required switching pulses and determines the shoot-through duration.

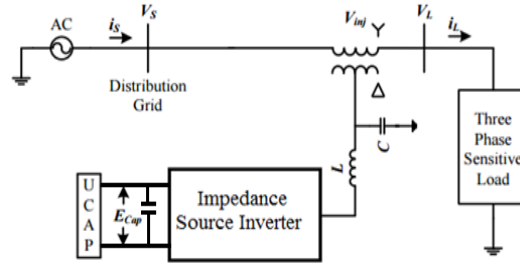


Figure 3. Proposed system

The voltage equation related with impedance network is (3)-(5):

$$V_{C1} = V_{C2} = V_C \tag{3}$$

$$V_{L1} = V_{L2} = V_L \tag{4}$$

$$B = \frac{1}{1 - 2 \frac{T_{shoot}}{T}} \tag{5}$$

where B-boost factor and T-switching frequency. The inverter's output peak ac voltage is expressed as (6):

$$\widehat{V}_{ac} = M \cdot B \cdot \frac{V_0}{2} \tag{6}$$

where the modulation index is M,  $V_0$  is the capacitor input voltage.

By controlling the boost factor and modulation index of the impedance network, the output voltage can be varied, and hence deep sags and swells can be cleared. A bidirectional switch is used instead of a diode, and it is closed during the active state and open during the shoot-through state. The control circuit is shown as above in Figure 4.

The dq-control approach is used to identify voltage sags, then the identified signal is compared with a triangular carrier waveform to generate the required switching pulses. Shoot-through states are introduced through a simple boost control algorithm, with the boost factor regulated by monitoring the DC link voltage in accordance with the depth of the sag. By appropriately coordinating the modulation index with the boost factor, a broad range of output voltage levels can be achieved. Consequently, during the occurrence of voltage sag and swell conditions, the proposed method is capable of significantly enhancing the overall power quality of the grid.

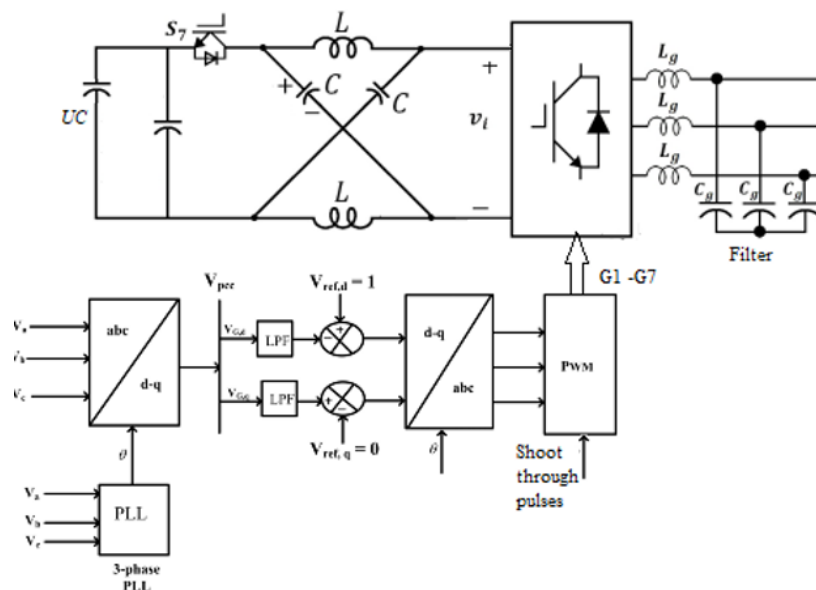


Figure 4. Control circuit of DVR

### 2.2.1. Proposed method with PI controller to control DC link voltage

A PI controller can be used to maintain DC link constant. If the DC-link voltage is stable and sustained at its reference value, the DVR can generate an accurate and continuous compensating voltage. The UCAP serves as the energy source, providing fast charging and discharging to supply or absorb the required power during voltage sags, swells, or transients. Therefore, DC-link voltage is constant through PI control, which ensures proper energy exchange between the UCAP and DVR, stable converter operation, and reliable voltage restoration, ultimately safeguarding sensitive loads from power quality issues.

### 2.2.2. Proposed method with MPC controller to control DC link voltage

Figure 5 illustrates the MPC control of shoot-through pulses. MPC evaluates different possible control actions and selects the one that reduces a cost function, typically defined to reduce the deviation of DC-link voltage compared to the reference value while also considering system constraints such as current and switching limits. This predictive and optimization-based approach enables precise and robust regulation of the DC-link voltage, especially under fast load variations and dynamic operating conditions, making it more effective than traditional PI-based controllers.

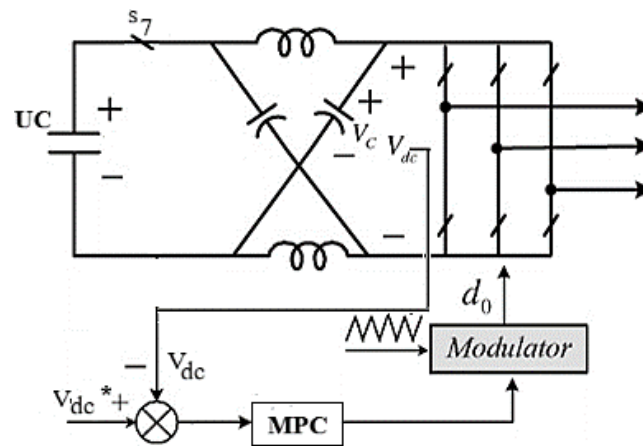


Figure 5. DC link control using MPC

## 3. RESULTS AND DISCUSSION

The sag and swell modes of voltage source-fed DVR with a bidirectional DC-DC converter and bidirectional impedance inverter are simulated. The parameters of the system employed in this investigation are listed in Table 1. An 11 kV, 50 Hz grid system provides 1.5 kW of power to the load using an 11 kV/400 V transformer. In 0.1–0.3 seconds, the system experiences 70% swell and 50% sag. MATLAB/Simulink is used to analyze the DVR's sag and swell situations.

### 3.1. VSI with BDC

In the first case, VSI-BDC, a voltage sag of 50% is created in the system, and the sag is detected using the vector control method. The PLL continuously tracks phase angle and supply voltage frequency, providing a reference for the synchronous reference frame (d–q transformation). The conversion from three-phase quantities (abc) to the rotating d–q frame is accurate, allowing precise separation of active (d-axis) and reactive (q-axis) components. By controlling these components independently, the reference signal for generating PWM for the inverter is generated. Without PLL, the DVR would not be able to align its reference frame with the grid, which would result in poor compensation performance during disturbances like sags, swells, or unbalances. The inverter draws energy from UCAP through a bidirectional converter and injects the missing voltage. UCAP discharges through BDC to the DC link of VSI. In Figure 6, plots of the voltage sag are presented for 50% sag between 0.1 and 0.3 s, and it can be observed that total harmonic distortion (THD) is improved to 3.75%. The experiment demonstrates that the VSI-BDC setup with vector control and PLL synchronization can mitigate a +70% voltage swell effectively in Figure 7. Load-side voltage is restored within acceptable tolerance in less than 10 ms, the DC-link remains stable, and THD is improved to 8.24%.

Table 1. Source parameters

| Parameters          |                       | Value              |
|---------------------|-----------------------|--------------------|
| Source parameters   | Fundamental frequency | 50 Hz              |
|                     | Source voltage        | 11 KV (L-L, rms)   |
| Load parameters     | Sensitive load        | 1.5 kW             |
| DVR                 | Filter inductor       | 6 mH               |
|                     | Filter capacitor      | 20 $\mu$ F         |
|                     | Transformer rating    | 1.5 kVA            |
|                     | Turns ratio           | 5/1                |
| Impedance converter | Capacitor (C1, C2)    | 100 $\mu$ F        |
|                     | Inductor (L1, L2)     | 0.833 mH           |
|                     | UCAP                  | 165 F, 48 V, 3 nos |

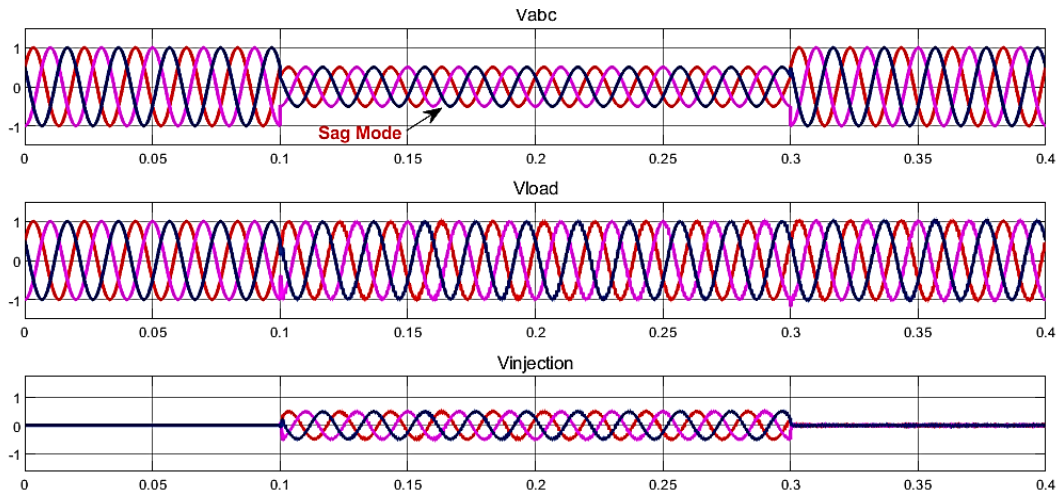


Figure 6. VSI with a bidirectional DC-DC converter during sag

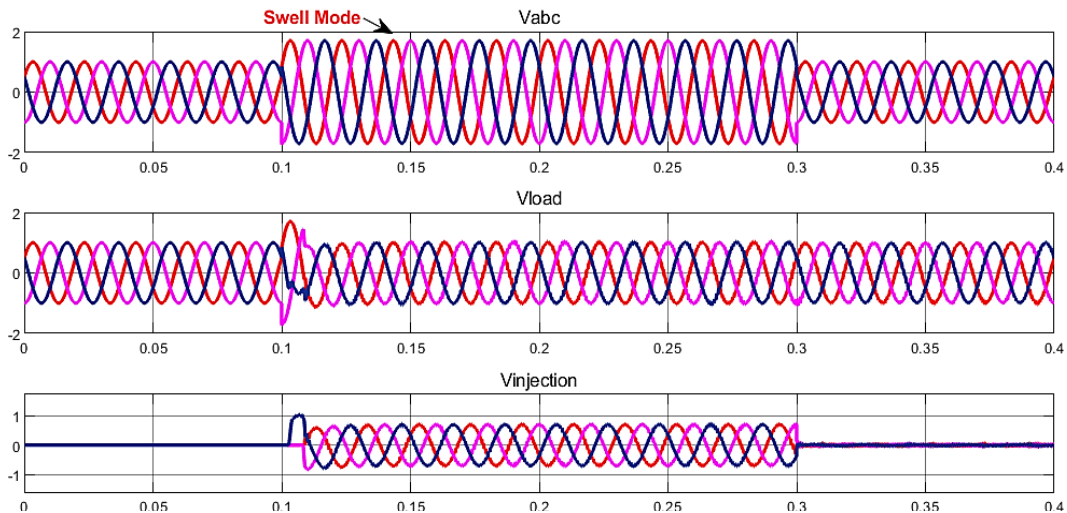


Figure 7. VSI with a bidirectional DC-DC converter during swell

### 3.2. Bidirectional ZSI-based DVR

#### 3.2.1. Without DC link voltage control

In this case, the DVR was tested under different grid disturbance conditions without employing active DC-link voltage control. A 50% voltage sag and a 70% swell were applied at point of common coupling (PCC) for a duration of 0.2 s each. The DVR, using the bidirectional Z-source inverter topology, was able to inject compensating voltages through its series transformer to restore the load voltage close to the nominal value. Shoot through ratio was selected as 0.25 so that boost factor is 2 and UCAP 100 V boosted to 200 V in DC-link of inverter.

The simulation circuit of the bidirectional ZSI in the DVR system is given in Figure 8. The overall circuit typically includes a three-phase controlled AC source, step down transformer, and a load. Inside the sub circuit of DVR shown in Figure 8, impedance source inverter (ZSI) connected to UCAP, control circuit to generate pulses, filter, and series injection transformer are integrated.

The recorded waveforms in Figures 9 and 10 show that during both sag and swell conditions, the DVR successfully reduced the disturbance impact at the load terminals. THD of the load is improved to 3.35% in sag and 2.28% in swell. However, due to the absence of a DC-link regulation loop, the capacitor voltage of the Z-source network experienced significant fluctuations. The THD of the swell condition of VSI-BDC DVR and ZSI DVR are compared in Figure 11. The THD is improved from 8.24% to 2.28%. Thus, effectively mitigates the swell condition.

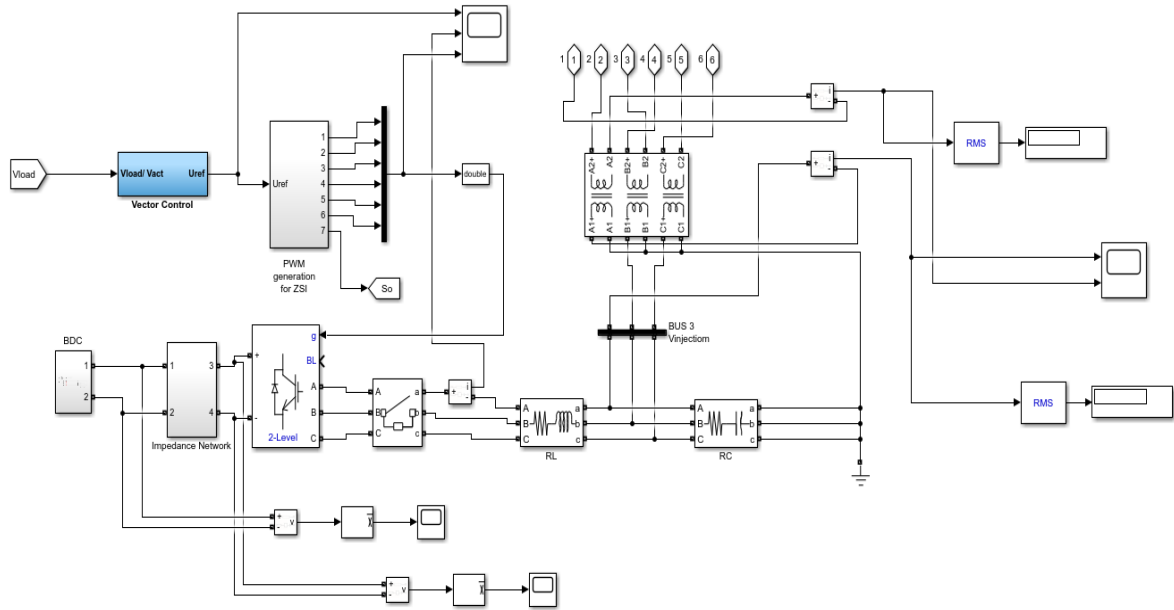


Figure 8. Simulation circuit of bidirectional ZSI

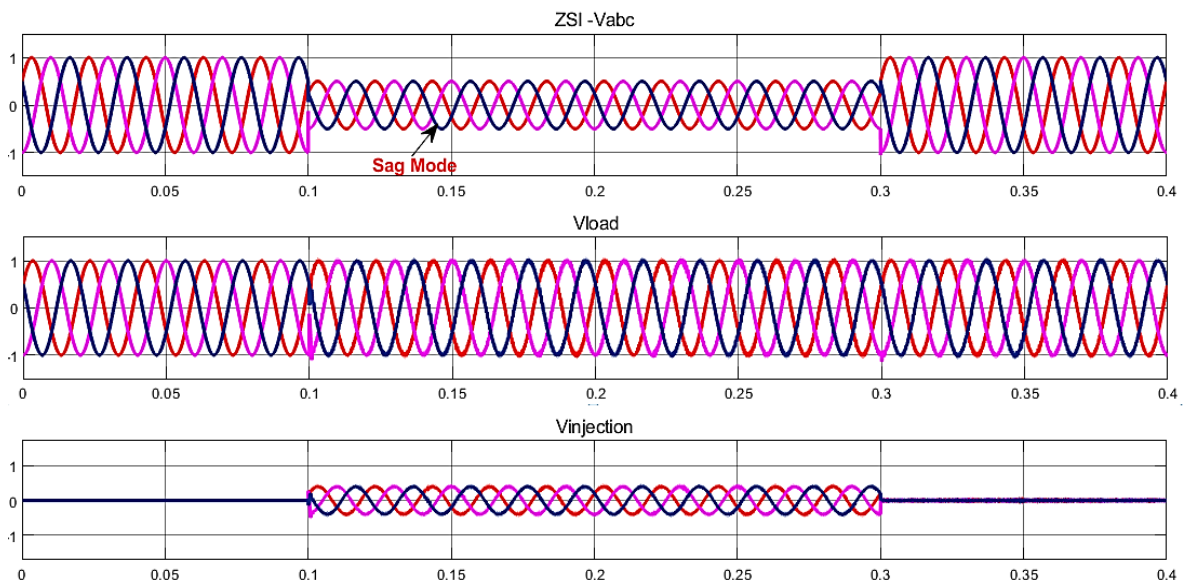


Figure 9. Bidirectional ZSI during sag

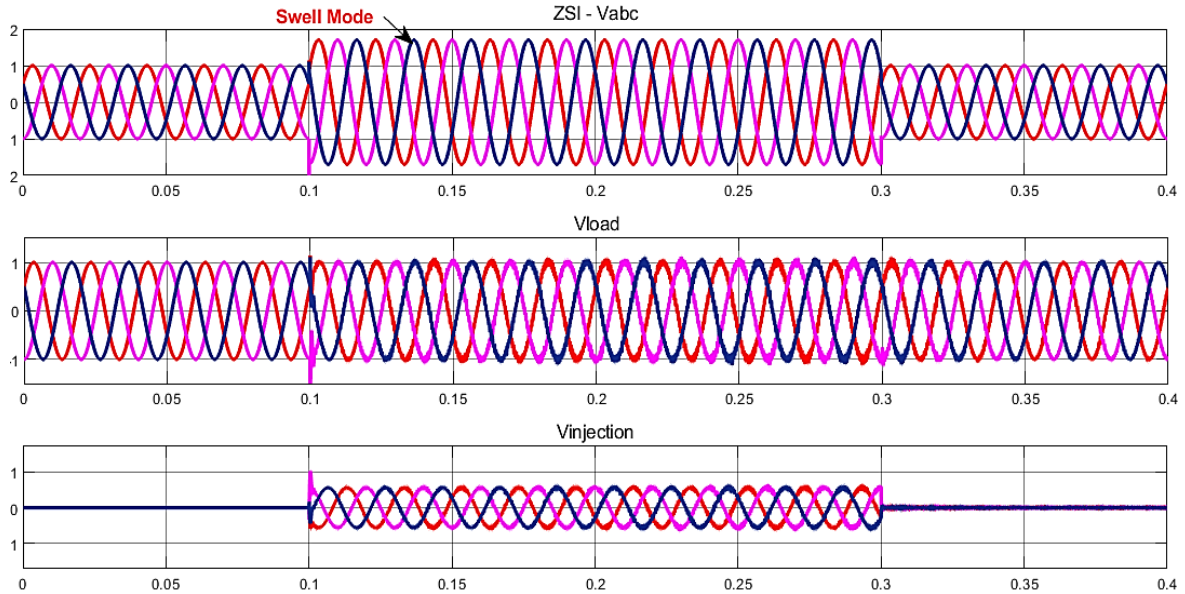


Figure 10. Bidirectional ZSI during swell

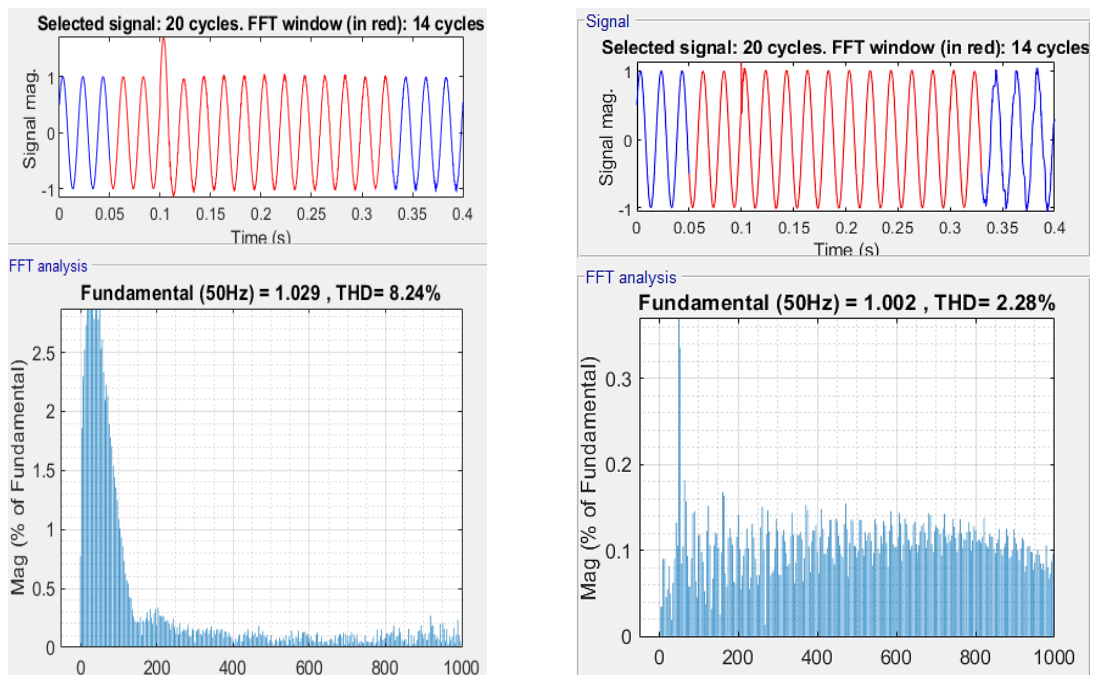


Figure 11. THD of VSI and ZSI swell

**3.2.2. With DC-link voltage control using PI controller**

In this case, the bidirectional ZSI-based DVR was tested with an active DC-link voltage control loop integrated into the system. The same disturbance conditions were applied as in the previous test: a 50% voltage sag and a 75% swell, each lasting 0.2s. Shoot through ratio are decided from the error signal of DC-link voltage. With the DC-link control enabled, the DVR demonstrated significantly improved dynamic performance and stability compared to the uncontrolled case as shown in Figure 12.

The measured results show that the load-side voltage was restored with THD of 2.69% and 2.25% during both sag and swell events. The injected compensation voltage closely followed the reference profile without overshoot, confirming precise control of the Z-source network. Importantly, the DC-link voltage was

maintained stable within  $\pm 2\%$  of its nominal value, preventing the capacitor over-voltage or under-voltage observed in the uncontrolled case.

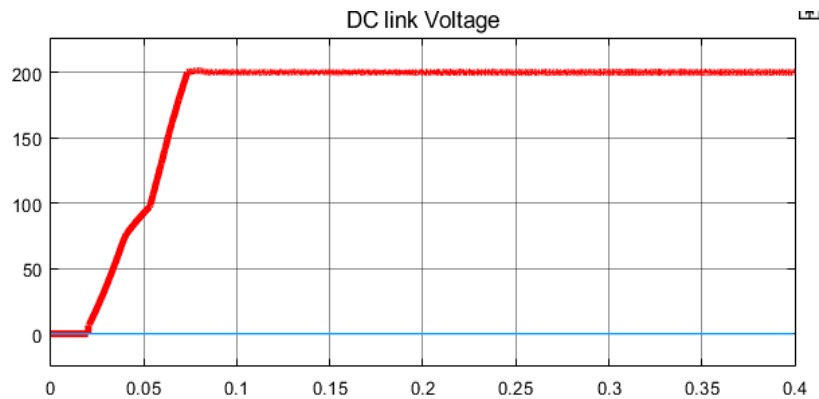


Figure 12. DC link voltage using PI controller

### 3.2.3. With DC-link voltage control using MPC controller

To further enhance the performance of the bidirectional ZSI-based DVR, a MPC strategy was implemented for DC-link voltage regulation. With MPC control, the DVR achieved superior transient response and voltage restoration compared to both the uncontrolled and PI-controlled cases. The recorded results show that the DVR compensated the disturbances effectively, maintaining the load voltage within  $\pm 2.6\%$  of nominal during both sag and swell events.

The overall results are compared in Table 2. The results clearly indicate that the bidirectional ZSI structure outperforms the conventional VSI by providing lower harmonic distortion for both sag and swell conditions. Furthermore, incorporating advanced DC-link control enhances performance, with MPC-based control offering the best overall THD reduction, making it the most effective option among those compared.

Table 2. The performance of DVR

| Method                                         | THD-sag | THD-swell |
|------------------------------------------------|---------|-----------|
| BDC with VSI                                   | 3.75%   | 8.24%     |
| Bidirectional ZSI                              | 3.35%   | 2.28%     |
| Bidirectional ZSI with PI control for DC link  | 2.69%   | 2.25%     |
| Bidirectional ZSI with MPC control for DC link | 2.63%   | 2.1%      |

## 4. CONCLUSION

In this paper, the bidirectional impedance converter is used to integrate UCAP into the DVR's DC-link. Temporary voltage surges and sags are mitigated by this converter. These converters are used to handle load levelling, peak power needs, and short-duration blackouts. ZSI enables a broad range of operation and quick recovery during swell time, resulting in high gain voltage at the output during sag. During swell time, the THD of ZSI with a bidirectional converter is enhanced from 7.01 to 3.61%. UCAP is charging during the swell period and discharging during the sag period. The UCAP-DVR system has active power capabilities and automatically adjusts for transient sags and swells without relying on the grid. The combination of predictive switching and DC-link voltage regulation enables the DVR to deliver superior power quality to sensitive loads under dynamic grid disturbances.

## FUNDING INFORMATION

Authors state no funding involved.

## AUTHOR CONTRIBUTIONS STATEMENT

This journal uses the Contributor Roles Taxonomy (CRediT) to recognize individual author contributions, reduce authorship disputes, and facilitate collaboration.

| Name of Author | C | M | So | Va | Fo | I | R | D | O | E | Vi | Su | P | Fu |
|----------------|---|---|----|----|----|---|---|---|---|---|----|----|---|----|
| A. Anitha      | ✓ | ✓ | ✓  | ✓  | ✓  | ✓ |   | ✓ | ✓ | ✓ |    |    |   | ✓  |
| K. C. R. Nisha |   | ✓ |    |    |    | ✓ |   | ✓ | ✓ | ✓ | ✓  | ✓  |   |    |

C : **C**onceptualizationM : **M**ethodologySo : **S**oftwareVa : **V**alidationFo : **F**ormal analysisI : **I**nvestigationR : **R**esourcesD : **D**ata CurationO : **W**riting - **O**riginal DraftE : **W**riting - **R**eview & **E**ditngVi : **V**isualizationSu : **S**upervisionP : **P**roject administrationFu : **F**unding acquisition

## CONFLICT OF INTEREST STATEMENT

Authors state no conflict of interest.

## DATA AVAILABILITY

The authors confirm that the data supporting the findings of this study are available within the article.

## REFERENCES

- [1] A. Moghassemi and S. Padmanaban, "Dynamic voltage restorer (DVR): A comprehensive review of topologies, power converters, control methods, and modified configurations," *Energies*, vol. 13, no. 16, p. 4152, Aug. 2020, doi: 10.3390/en13164152.
- [2] N. Mbali, "Dynamic voltage restorer as a solution to voltage problems in power systems: Focus on sags, swells and steady fluctuations," *Energies*, vol. 16, no. 19, p. 6946, Oct. 2023, doi: 10.3390/en16196946.
- [3] A. H. Soomro *et al.*, "Enhancement of power quality based on dynamic voltage restorer matrix inverter-sliding mode control scheme," *Electric Power Systems Research*, vol. 241, p. 111408, Apr. 2025, doi: 10.1016/j.epr.2025.111408.
- [4] J. G. Nielsen and F. Blaabjerg, "A detailed comparison of system topologies for dynamic voltage restorers," *IEEE Transactions on Industry Applications*, vol. 41, no. 5, pp. 1272–1280, 2005, doi: 10.1109/TIA.2005.855045.
- [5] P. Jayaprakash, B. Singh, D. P. Kothari, A. Chandra, and K. Al-Haddad, "Control of reduced-rating dynamic voltage restorer with a battery energy storage system," *IEEE Transactions on Industry Applications*, vol. 50, no. 2, pp. 1295–1303, 2014, doi: 10.1109/TIA.2013.2272669.
- [6] A. M. Gee, F. Robinson, and W. Yuan, "A superconducting magnetic energy storage-emulator/battery supported dynamic voltage restorer," *IEEE Transactions on Energy Conversion*, vol. 32, no. 1, pp. 55–64, 2017, doi: 10.1109/TEC.2016.2609403.
- [7] D. Somayajula and M. L. Crow, "An integrated dynamic voltage restorer-ultracapacitor design for improving power quality of the distribution grid," *IEEE Transactions on Sustainable Energy*, vol. 6, no. 2, pp. 616–624, Apr. 2015, doi: 10.1109/TSTE.2015.2402221.
- [8] A. D. Falehi and M. Rafiee, "Optimal control of novel fuel cell-based DVR using ANFISC-MOSSA to increase FRT capability of DFIG-wind turbine," *Soft Computing*, vol. 23, no. 15, pp. 6633–6655, 2019, doi: 10.1007/s00500-018-3312-9.
- [9] M. S. Shah, T. Mahmood, and M. F. Ullah, "Power quality improvement using ultra capacitor based dynamic voltage restorer with real twisting sliding mode control," *Electrical Engineering and Electromechanics*, vol. 2022, no. 1, pp. 59–63, 2022, doi: 10.20998/2074-272X.2022.1.08.
- [10] P. A. A. Farzana, R. Ramchand, and H. S. Nair, "A survey of bidirectional DC-DC converters for transportation electrification and microgrid applications," *2023 International Conference on Power, Instrumentation, Control and Computing, PICC 2023*, 2023, doi: 10.1109/PICC57976.2023.10142639.
- [11] Y. P. Siwakoti, F. Z. Peng, F. Blaabjerg, P. C. Loh, and G. E. Town, "Impedance-source networks for electric power conversion Part I: A topological review," *IEEE Transactions on Power Electronics*, vol. 30, no. 2, pp. 699–716, 2015, doi: 10.1109/TPEL.2014.2313746.
- [12] S. Sajadian and R. Ahmadi, "ZSI for PV systems with LVRT capability," *IET Renewable Power Generation*, vol. 12, no. 11, pp. 1286–1294, 2018, doi: 10.1049/iet-rpg.2018.5104.
- [13] O. Ellabban, J. Van Mierlo, and P. Lataire, "Control of a bidirectional z-source inverter for electric vehicle applications in different operation modes," *Journal of Power Electronics*, vol. 11, no. 2, pp. 120–131, 2011, doi: 10.6113/JPE.2011.11.2.120.
- [14] J. Rąbkowski, "The bidirectional Z-source inverter as an energy storage/grid interface," *EUROCON 2007 - The International Conference on Computer as a Tool*, pp. 1629–1635, 2007, doi: 10.1109/EURCON.2007.4400641.
- [15] V. Sharma, M. J. Hossain, and S. Mukhopadhyay, "Fault-tolerant operation of bidirectional ZSI-Fed induction motor drive for vehicular applications," *Energies*, vol. 15, no. 19, 2022, doi: 10.3390/en15196976.
- [16] P. C. Loh, D. M. Vilathgamuwa, Y. Sen Lai, G. T. Chua, and Y. Li, "Pulse-width modulation of Z-source inverters," *Conference Record - IAS Annual Meeting (IEEE Industry Applications Society)*, vol. 1, pp. 148–155, 2004, doi: 10.1109/ias.2004.1348401.
- [17] S. D. Dehnavi, C. Negri, S. Bayne, and M. Giesselmann, "Dynamic voltage restorer (DVR) with a novel robust control strategy," *ISA Transactions*, vol. 121, pp. 316–326, 2022, doi: 10.1016/j.isatra.2021.04.010.
- [18] Y. Li, Y. Shi, Z. Hu, C. Zou, and Q. Lei, "Two-stage DVR control with improved dynamic performance under nonlinear load condition," *2022 4th International Conference on Smart Power and Internet Energy Systems, SPIES 2022*, pp. 984–989, 2022, doi: 10.1109/SPIES55999.2022.10082412.
- [19] M. İnci, K. Ç. Bayindir, and M. Tümay, "The performance improvement of dynamic voltage restorer based on bidirectional DC-DC converter," *Electrical Engineering*, vol. 99, no. 1, pp. 285–300, 2017, doi: 10.1007/s00202-016-0422-1.
- [20] M. M. Savrun, T. Koroğlu, A. Tan, M. U. Cuma, K. Ç. Bayindir, and M. Tümay, "Isolated H-bridge DC-DC converter integrated transformerless DVR for power quality improvement," *IET Power Electronics*, vol. 13, no. 5, pp. 920–926, 2020, doi: 10.1049/iet-pel.2019.0687.

- [21] N. Mallick and V. Mukherjee, "Self-tuned fuzzy-proportional-integral compensated zero/minimum active power algorithm based dynamic voltage restorer," *IET Generation, Transmission & Distribution*, vol. 12, no. 11, pp. 2778–2787, Jun. 2018, doi: 10.1049/iet-gtd.2017.1170.
- [22] T. A. Naidu, S. R. Arya, and R. Maurya, "Multiobjective dynamic voltage restorer with modified EPLL control and optimized pi-controller gains," *IEEE Transactions on Power Electronics*, vol. 34, no. 3, pp. 2181–2192, Mar. 2019, doi: 10.1109/TPEL.2018.2837009.
- [23] T. A. Naidu, S. R. Arya, R. Maurya, and S. Padmanaban, "Performance of DVR using optimized PI controller based gradient adaptive variable step LMS control algorithm," *IEEE Journal of Emerging and Selected Topics in Industrial Electronics*, vol. 2, no. 2, pp. 155–163, Apr. 2021, doi: 10.1109/JESTIE.2021.3051553.
- [24] R. V. Rao, "Rao algorithms: Three metaphor-less simple algorithms for solving optimization problems," *International Journal of Industrial Engineering Computations*, pp. 107–130, 2020, doi: 10.5267/j.ijiec.2019.6.002.
- [25] D. Liu, H. Zhang, X. Liang, and S. Deng, "Model predictive control for three-phase, four-leg dynamic voltage restorer," *Energies*, vol. 17, no. 22, p. 5622, Nov. 2024, doi: 10.3390/en17225622.

## BIOGRAPHIES OF AUTHORS



**A. Anitha**    received her B.E. degree in Electrical and Electronics Engineering from Kumaraguru College of Technology, Coimbatore, in 2004. She received M.E. in Power Electronics and drives from Government College of Technology in 2006. She is working as a senior assistant professor in the Department of Electrical and Electronics Engineering, New Horizon College of Engineering, Bangalore. Currently, she is pursuing a Ph.D. in New Horizon College of Engineering, Bangalore, Visvesvaraya Technological University, Belagavi, Karnataka, India. Her research interest includes power electronics controllers and power quality. She can be contacted at email: anithanelson24@gmail.com.



**K. C. R. Nisha**    received her B.E. degree in Electronics and Communication Engineering from Bharathidasan University, Trichy in 2002. She received an M.E. in Power Electronics and a Ph.D. in Power Converters for Renewable Energy Systems from Sathyabama University, Chennai, in 2004 and 2015, respectively. She started her career as a lecturer at Sathyabama University (2003-2009). She joined New Horizon College of Engineering, Bangalore, in 2009 and is currently working as a professor at the Department of Electronics and Communication Engineering. She has more than 16 years of academic cum research experience at the university and college level. Her contributions are recognized in the field of efficient power converters for renewable energy systems and embedded control of power applications. She is currently vice chair of the IEEE Industrial Electronics Society - Bangalore chapter (IES 2021), publication chair-joint IEEE PEL/IES Bangalore chapter (2021), point of contact (PoC) for UNISEC India Local Chapter Bangalore Section, ISRO -IIRS Coordinator of NHCE Student branch, counsellor of NHCE IEEE, and MTS NHCE chapters. She can be contacted at email: nishashaji@gmail.com.